Macromolecules
ARTICLE

Macromolecules **2010**, *43*, 5417–5423 **5417**
DOI: 10.1021/ma902804e

Effect of an Ionic Liquid Solvent on the Phase Behavior of Block Copolymers

Justin M. Virgili,[†,‡,⊥] Megan L. Hoarfrost,[†,§,⊥] and Rachel A. Segalman*[,†,‡]

[†]*Department of Chemical Engineering, University of California, Berkeley, California 94720,* [‡]*Materials Sciences, and* [§]*Energy and Environmental Technologies Divisions, Lawrence Berkeley National Laboratory, Berkeley, California 94720.* [⊥] *Authors contributed equally*

Received December 19, 2009; Revised Manuscript Received March 31, 2010

ABSTRACT: The phase behavior of concentrated mixtures of block copolymers with an ionic liquid has been studied using a large series of block copolymers with varying molecular weight and volume fraction to gain a thorough understanding of the thermodynamics of self-assembly. The lyotropic phase behavior of mixtures of poly(styrene-*block*-2-vinylpyridine) (S2VP) copolymers with the ionic liquid imidazolium bis(trifluoromethane)sulfonimide ([Im][TFSI]) is reminiscent of block copolymer/selective molecular solvent mixtures, and ordered microstructures corresponding to lamellae, hexagonally close-packed cylinders, body-centered cubic, and face-centered cubic oriented micelles are observed. Scaling analysis reveals that, in contrast to observations of block copolymer/molecular solvent mixtures, the interfacial area occupied by each S2VP chain decreases upon the addition of [Im][TFSI], indicating a considerable increase in the effective segregation strength of the S2VP copolymer with ionic liquid addition.

Introduction

Ionic liquids are an exciting class of materials due to unique properties including high thermal and electrochemical stability, negligible volatility, and high ionic conductivity.[1] This exceptional combination of properties makes them candidates for a variety of applications such as fuel cells,[2−6] transistors,[7,8] and battery electrolytes,[9,10] for which it would be desirable to integrate the ionic liquid into a solid polymeric matrix. Such a material can be realized by selectively incorporating the ionic liquid into a continuous block copolymer phase, forming a membrane in which the second phase provides mechanical stability.[11] Fundamental understanding of block copolymer/ionic liquid interactions and the resulting self-assembly is essential for predictable structure and property control.

Both "solvent-like" and "salt-like" properties of an ionic liquid have been observed in block copolymer/ionic liquid mixtures.[12] Addition of a molecular solvent to a block copolymer typically results in lyotropic phase transitions, changes in characteristic domain spacing (d), and changes in the order−disorder transition temperature (T_{ODT}).[13−18] In the case of block copolymer/salt mixtures, changes in the phase behavior relative to the neat copolymer have been interpreted as changes in the effective segregation strength, chain statistics, or intermolecular coordination.[19−22] Recently, Wang has developed an analytical expression for an effective interaction parameter, χ_{eff}, in homopolymer blend/salt mixtures that incorporates ion solvation and entropic effects.[23] Previous experimental studies of the self-assembly of dilute[24] and concentrated[11] poly(1,2-butadiene-*block*-ethylene oxide)/ionic liquid mixtures have highlighted the similarity of the phase behavior of the mixtures to that of block copolymer/molecular solvent mixtures. However, studies of the thermal properties of poly(styrene-*block*-2-vinylpyridine) (S2VP)/ionic liquid mixtures have shown an increased glass transition temperature (T_g) of the poly(2-vinylpyridine) (P2VP) phase at low ionic liquid concentrations due to a salt-like physical cross-linking, while at high ionic liquid concentrations the T_g of the P2VP block was depressed as it would be in the presence of a molecular solvent.[12]

In this work the effect of block copolymer volume fraction, f_{PS}, and degree of polymerization, N_T, on the phase behavior of concentrated S2VP copolymer mixtures with the ionic liquid imidazolium bis(trifluoromethane)sulfonimide ([Im][TFSI]) (Figure 1) is explored to gain a thorough understanding of the thermodynamics of self-assembly in this complex system. In particular, thermal characterization of S2VP/[Im][TFSI] mixtures reveals an unusual composition dependence of T_g not predicted by either the Gordon−Taylor or Fox equations for polymer/molecular solvent mixtures. The lyotropic phase behavior of the mixtures is studied using small-angle X-ray scattering (SAXS) and small-angle neutron scattering (SANS) and compared to that of mixtures of block copolymers in selective molecular solvents. Scaling analysis of the structural length scales and studies of the thermotropic phase behavior of the S2VP/[Im][TFSI] mixtures reveal a substantial increase in segregation strength upon the addition of ionic liquid compared to block copolymer/selective molecular solvent mixtures. It is anticipated that the increased segregation strength is due to the enthalpic driving force for ions to reside in the high dielectric P2VP phase of the block copolymer.[23]

Experimental Section

Polymer Synthesis and Characterization. S2VP copolymers and P2VP homopolymer were synthesized via anionic polymerization using standard methods.[25] The molecular weight of the polystyrene (PS) hompolymer was determined using gel permeation chromatography (GPC), and the total molecular weight of the block copolymer was determined via ^{1}H NMR (Bruker AVB-300). The molecular weight of the P2VP homopolymer was determined using ^{1}H NMR end-group analysis. The polydispersity of each polymer was assessed using GPC. The S2VP copolymers are designated S2VP($xx-yy$) and the P2VP

*Corresponding author. E-mail: segalman@berkeley.edu.

Published on Web 05/26/2010

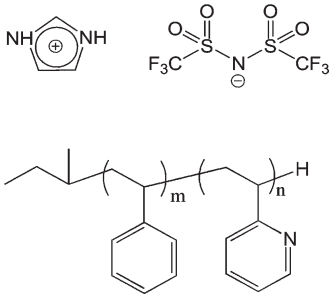

Figure 1. Chemical structures of imidazolium and TFSI ions and poly(styrene-*block*-2-vinylpyridine) copolymer.

homopolymer is designated P2VP(*yy*), where "*xx*" and "*yy*" refer to the number-averaged molecular weights in kg/mol of the PS and P2VP blocks, respectively. The total molecular weight, volume fraction of polystyrene, f_{PS}, and polydispersity index (PDI) of the polymers are given in Table 1. One of the 10 polymers, *d*S2VP(7.1−6.8) was synthesized with d_8-styrene monomer obtained from Polymer Source.

Ionic Liquid Purification. Imidazole (≥95%) and bis(trifluoromethane)sulfonimide (HTFSI, ≥95%) were purchased from Sigma-Aldrich and purified by sublimation under vacuum. Differential scanning calorimetry (DSC) and ^{1}H NMR were used to assess the purity of the two starting materials. Purified imidazole and HTFSI were combined in equimolar quantities in a glovebox, sealed in a glass vial, and heated in an oven outside the glovebox to 100 °C for 2−3 h to prepare the ionic liquid [Im][TFSI]. The composition of the ionic liquid was confirmed by comparing the measured melting point of the compound with literature.[2] Care was taken to limit air and water exposure of the hydroscopic ionic liquid by handling the material in an argon glovebox and sealed sample holders.

Scattering Sample Preparation and Methods. Dichloromethane was degassed using three freeze−pump−thaw cycles, stirred over CaH_2 overnight, then distilled into a collection flask, brought into a glovebox, and stored on molecular sieves. All further sample preparation was performed within an argon glovebox. Predetermined quantities of [Im][TFSI] and S2VP were weighed into glass vials, ca. 5 wt % solutions were prepared by dissolution in dichloromethane, and the solutions were stirred overnight. Samples were cast one drop at a time into sample cells formed by an aluminum spacer sealed onto a Kapton (SAXS) or quartz (SANS) window on one side until a ca. 1 mm solid sample was obtained. Samples were heated to 60 °C (above the boiling point of dichloromethane) for ca. 18 h to remove remaining solvent. A second Kapton (SAXS) or quartz (SANS) window was glued to seal the samples. Samples were sealed in jars containing desiccant in the argon glovebox for transportation to the beamline. Samples are designated by the value of the polymer volume fraction, ϕ_P, assuming ideal mixing. The density of [Im][TFSI] was estimated to be 1.67 g/cm^3 from scattering length density fits of SANS intensity profiles,[26] and the densities of hydrogenated PS, deuterated PS, and P2VP were taken to be 1.05, 1.12 and 1.05 g/cm^3, respectively.

SAXS was performed on beamline 7.3.3 of the Advanced Light Source (ALS) and beamline 1-4 of the Stanford Synchrotron Radiation Lightsource (SSRL). At the ALS, the beamline was configured with an X-ray wavelength of $\lambda = 1.240$ Å and focused to a 50 by 300 μm spot. Samples were equilibrated on the beamline at 145 °C for 20−30 min before data were gathered. Full two-dimensional scattering patterns were collected on an ADSC CCD detector with an active area of 188 by 188 mm. The scattering patterns were radially averaged, and the scattering intensity was corrected with the postion chamber intensity using Nika version 1.18. At the SSRL, the beamline was configured with an X-ray wavelength $\lambda = 1.488$ Å and focused to a 0.5 mm diameter spot. A single quadrant of a two-dimensional scattering pattern was collected on a CCD detector with an active area of 25.4 by 25.4 mm. The scattering patterns were radially averaged and corrected for detector null signal, dark current, and empty cell scattering.

Table 1. Characteristics of Block Copolymers Studied

sample	total MW (g/mol)	f_{PS}	PDI
	constant N_T		
S2VP(4.4−10.8)	15 200	0.29	1.07
S2VP(4.9−6.6)	11 500	0.43	1.13
*d*S2VP(7.1−6.8)	13 900	0.50	1.10
	constant N_{P2VP}		
P2VP(13.1)	13 100	0.00	1.06
S2VP(8.7−12.0)	20 800	0.42	1.02
S2VP(12.0−12.4)	24 300	0.49	1.19
S2VP(18.4−11.4)	29 800	0.62	1.10
S2VP(28.5−10.7)	39 200	0.73	1.04

SANS measurements of mixtures of *d*S2VP(7.1−6.8) with [Im][TFSI] were performed at Oak Ridge National Laboratory on the SANS-I instrument. Neutrons with a $\lambda = 6.0$ Å wavelength and a sample-to-detector distance of 4 and 10 m were utilized. Data from room temperature samples were collected, and the intensity was corrected for instrumental background, empty cell scattering, sample transmission, and incoherent background and placed on an absolute intensity scale by use of a porous carbon standard (Al4).[27] In some samples, a small positive scattering intensity, typically on the order of 0.1 cm^{-1}, remained after this data reduction procedure, likely due to incoherent scattering.[28] In these cases, the residual intensity was removed by subtracting the average intensity over the range $0.085 < q < 0.100$ Å^{-1}.

Differential Scanning Calorimetry Sample Preparation and Methods. Differential scanning calorimetry (DSC) was performed on a TA Instruments DSC 2920. Samples were solution cast in a glovebox into aluminum DSC pans from the same solutions used to prepare scattering samples. The samples were heated to 60 °C for ca. 18 h to remove remaining solvent. The samples were then crimped within the glovebox using hermetically sealed pans and placed inside a container with desiccant for transfer to the DSC. Indium and dodecane were used as calibration standards for the DSC. Samples underwent three heating and cooling cycles and glass transitions recorded upon the second heating were reported.

Results and Discussion

Thermal Properties of S2VP/[Im][TFSI] System. The thermal properties of S2VP/[Im][TFSI] mixtures highlight the complex effect of the addition of an ionic liquid to a block copolymer. In the neat S2VP copolymers, a single T_g is observed in the vicinity of 100 °C due to the similarity of the T_g of the PS and P2VP homopolymers. While the T_g of the PS phase remains in the viscinity of 100 °C upon the addition of ionic liquid, the presence of a sufficient amount of ionic liquid (>4 wt %) leads to a decrease in the T_g of the P2VP-rich phase due to the high selectivity of [Im][TFSI] for this phase.[26] In Figure 2, the low temperature T_g is plotted as a function of weight fraction of ionic liquid in the P2VP-rich phase, w_{IL} (where w_{IL} and w_{P2VP} sum to one), assuming all ionic liquid partitions into the P2VP-rich phase. Representative differential scanning calorimetry (DSC) scans, used to determine the T_g of the PS and P2VP phases of the mixtures, are included in Supporting Information, Figure S1. The ratio of [Im][TFSI] to P2VP is found to be predictive of the P2VP/[Im][TFSI] T_g, regardless of the f_{PS} and N_T of the S2VP copolymers, as indicated by the collapse of the data onto a single curve. The Gordon−Taylor[29] and Fox[30] equations (eqs 1 and 2, respectively) have been routinely used to

describe the T_g of polymer/molecular solvent mixtures and polymer ion gels[31] and are given by

$$T_g = v_{IL} T_{g,IL} + v_{P2VP} T_{g,P2VP} \quad (1)$$

$$\frac{1}{T_g} = \frac{w_{IL}}{T_{g,IL}} + \frac{w_{P2VP}}{T_{g,P2VP}} \quad (2)$$

where v_{P2VP} and v_{IL} are the volume fractions of P2VP and [Im][TFSI] in the P2VP/[Im][TFSI] phase. The T_g of [Im][TFSI] is below the range of our DSC (−40 to 725 °C) and also not available from the literature. Thus, the [Im][TFSI] T_g was used as a fitting parameter to compare eqs 1 and 2 to the P2VP/[Im][TFSI] T_g data. Neither the Gordon−Taylor nor the Fox equations capture the composition dependence of the T_g data. Both equations predict a monotonically decreasing relationship between the T_g of a polymer and the solvent weight or volume fraction with a concave-up curve shape. In contrast, an unusual concave-down curve shape is observed in Figure 2. It is conceivable that specific interactions between [Im][TFSI] and P2VP that are not captured by the Gordon−Taylor or the Fox equations lead to the unique composition dependence of the T_g of the P2VP phase observed in Figure 2.

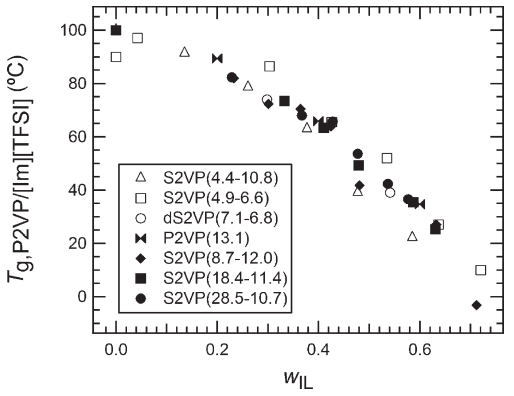

Figure 2. T_g of the P2VP/[Im][TFSI] phase as a function of w_{IL} determined using DSC.

Lyotropic Phase Behavior. The phase behavior of mixtures of [Im][TFSI] with two series of S2VP copolymers, one with constant N_T and one with constant N_{P2VP} (Table 1), demonstrates the similarity between mixtures of block copolymers with a selective molecular solvent and mixtures with an ionic liquid. Representative SAXS profiles are shown in Figure 3 from mixtures of S2VP copolymers of both series with [Im][TFSI] to highlight specific lyotropic phase transitions. Additional SAXS and SANS data are included in Supporting Information Figures S2 and S3, and Figure S4 features expanded SAXS profiles such that detailed higher order peaks and other subtle features are more clearly visible. In Figure 3a, the neat S2VP(4.4−10.8) copolymer with f_{PS} = 0.29 exhibits a hexagonally close-packed (HCP) cylinder morphology with a domain spacing (d) of 14.9 nm (110 scattering plane). As expected, the addition of ionic liquid (ϕ_P = 0.95−0.48) increases d, indicating that [Im][TFSI] acts as a selective solvent in the S2VP copolymer.[12] At a composition of ϕ_P = 0.42, the higher order scattering peaks reveal a lyotropic transition to spheres packed on a body-centered cubic (BCC) lattice. The presence of the $\sqrt{7}q^*$ scattering peak as well as the higher scattering intensity of the $\sqrt{3}q^*$ peak compared to the $\sqrt{2}q^*$ peak differentiates the observed SAXS profile from that of spherical micelles oriented on a

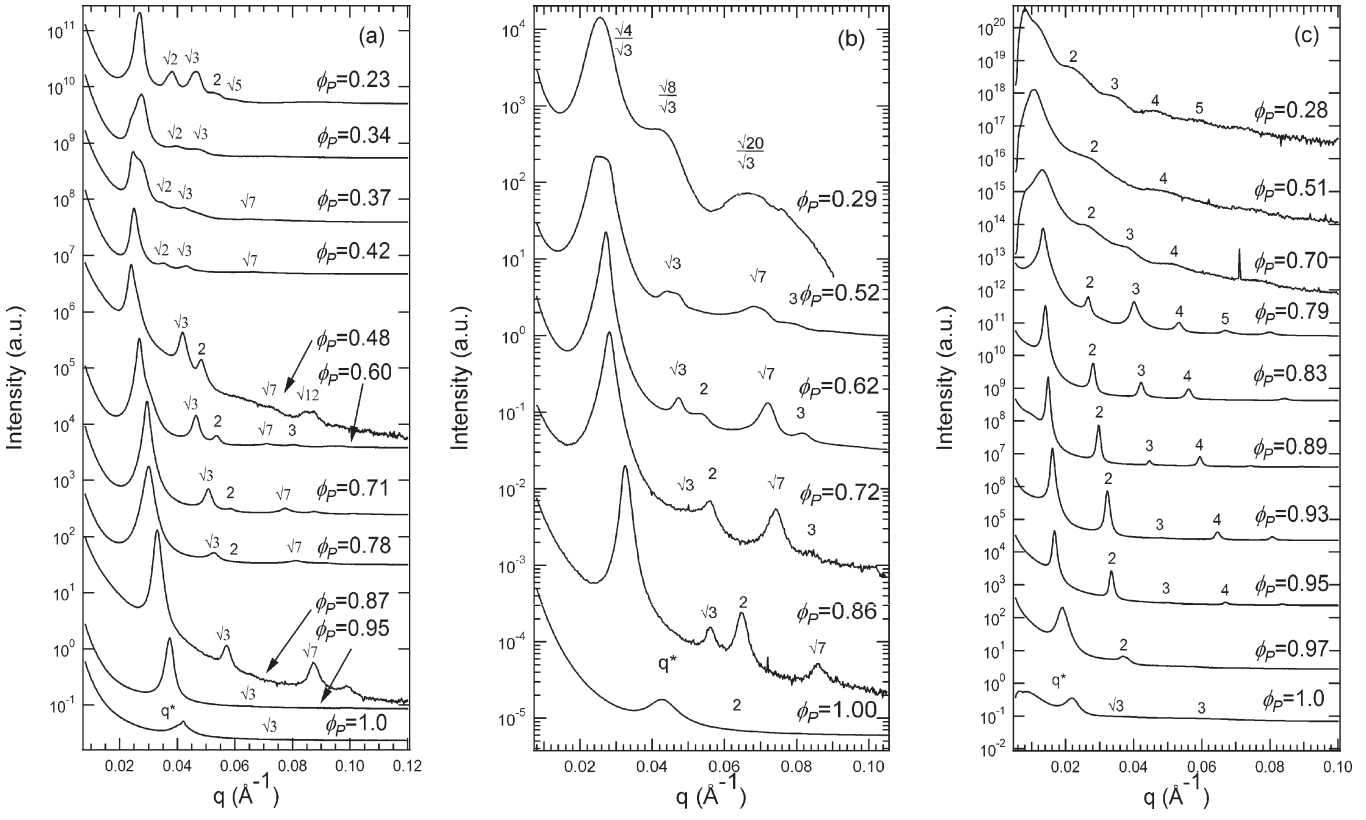

Figure 3. SAXS profiles of varying ϕ_P for (a) S2VP(4.4−10.8), (b) S2VP(4.9−6.6), and (c) S2VP(28.5−10.7) copolymers. In all cases, peak labels correspond to the q/q^* for scattering peaks and the profiles are recorded at 145 °C.

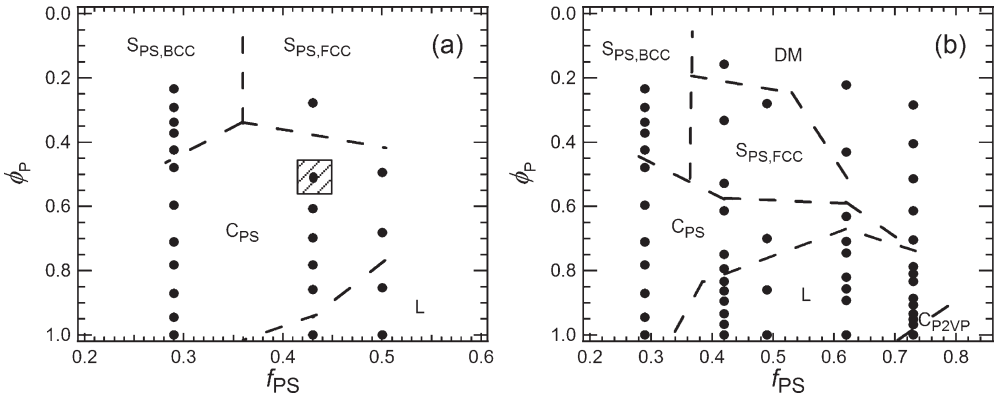

Figure 4. Lyotropic phase diagrams of S2VP/[Im][TFSI] mixtures for (a) fixed N_T and (b) fixed N_{P2VP} at T = 145 °C. Markers indicate phases identified using small-angle scattering, and dashed lines are drawn to indicate interpolated phase boundaries. Regions of coexistence are indicated with diagonal shading. Phases are labeled as follows: lamellae (L), HCP PS cylinders (C_{PS}), HCP P2VP cylinders (C_{P2VP}), FCC and BCC PS spheres ($S_{PS,FCC}$ and $S_{PS,BCC}$, respectively), and micelles with liquidlike order (DM).

simple cubic (SC) lattice.[32] It appears that the coexistence window required by Gibb's phase rule between the two phases is small ($\Delta\phi_P \leq 0.06$).[33] As ϕ_P is decreased to ϕ_P = 0.37 and ϕ_P = 0.34, distinct shoulders are observed on the primary scattering peak. At ϕ_P = 0.23 the q^* peak narrows and the higher order scattering peaks corresponding to BCC-packed spheres persist, indicating that the ϕ_P = 0.34 and ϕ_P = 0.37 mixtures consist of coexisting BCC-packed spheres with slightly incommensurate unit cells. This finding suggests that long equilibration times are necessary for the formation of stable, ordered micellar structures in block copolymer/ionic liquid mixtures,[34] and that the driving force for recovery of micellar phases at non-equilibrium lattice spacings is exceedingly small.[35]

In a more nearly symmetric S2VP(4.9−6.6) copolymer with f_{PS} = 0.43 the neat lamellar structure swells to form a HCP cylinder phase when $0.62 \leq \phi_P \leq 0.86$ (Figure 3b). At ϕ_P = 0.52, a distinctive broadening of the q^*, $\sqrt{3}q^*$, $\sqrt{7}q^*$, and $3q^*$ scattering peaks suggests a lyotropic transition; however, the likelihood of coexistence makes phase identification impossible. Upon further decreasing ϕ_P to ϕ_P = 0.29, reflections at $\sqrt{3}q^*$, $\sqrt{4}q^*$, $\sqrt{8}q^*$, and $\sqrt{20}q^*$ are observed corresponding to a lyotropic transition to PS spheres on a face-centered cubic (FCC) lattice.

Figure 3c illustrates the qualitative differences in the lyotropic phase behavior of copolymers with a PS majority phase. The HCP P2VP cylinders observed in the neat f_{PS} = 0.73 S2VP(28.5−10.7) copolymer undergo a lyotropic phase transition to a lamellar microstructure at ϕ_P = 0.95. At ϕ_P = 0.70, a dramatic broadening of the q^* peak is observed along with weak, undulating higher order scattering peaks revealing micelles with liquidlike order (DM) that persist as ϕ_P is further reduced to ϕ_P = 0.28. The asymmetry of the PS and P2VP blocks in the f_{PS} = 0.73 S2VP(28.5−10.7) copolymer likely leads to packing frustration in the PS phase upon addition of ionic liquid, which disrupts the formation of long-range order ($\phi_P \leq 0.70$). These findings demonstrate the rich variety of microstructures attainable in S2VP/[Im][TFSI] mixtures through modification of f_{PS}, N, and ϕ_P. Further, from the sequence of lyotropic phase transitions observed in the f_{PS} = 0.29, 0.43, and 0.73 copolymers it is evident that the [Im][TFSI] ionic liquid selectively solvates the P2VP block.

Lyotropic phase diagrams of the S2VP/[Im][TFSI] mixtures for the series of S2VP copolymers with constant N_T and N_{P2VP} demonstrate similarities to the lyotropic phase behavior of block copolymer/selective molecular solvent mixtures (Figure 4). For example, spheres on a BCC lattice are both predicted and experimentally observed in selective solvent/block copolymer systems in which the corona layer is large relative to the core[14,32,36] and are also observed in mixtures containing S2VP(4.4−10.8) (f_{PS} = 0.29) at low ϕ_P. For "inverted spheres", in which the corona is small relative to the core, FCC and BCC packings have been predicted and observed for block copolymer/selective solvent systems.[14,15] Block copolymers with thin corona layers in the most highly selective solvents for the corona tend to form FCC-packed spheres, which is consistent with the behavior of mixtures containing the compositionally symmetric S2VP(4.9−6.6) and S2VP(8.7−12.0) copolymers with [Im][TFSI]. For $f_{PS} \geq 0.42$, micelles with liquidlike order are observed in mixtures with the lowest values of ϕ_P characterized. The concentration range for the DM structures increases with increasing f_{PS}, similar to observations in molecular solvent systems.[11,37,38]

The lyotropic phase diagrams describing S2VP/[Im][TFSI] mixtures for constant N_T (Figure 4a) and constant N_{P2VP} (Figure 4b) are compared to determine the effect of block copolymer degree of polymerization on self-assembly. The lyotropic phase behavior of the constant N_T series and N_{P2VP} series are qualitatively similar with the notable exception of the narrower ϕ_P window between lamellar and micellar phases in the N_{P2VP} series. As the PS blocks of the copolymers in the constant N_{P2VP} series systematically have a higher degree of polymerization at a given f_{PS} than those in the constant N_T series, the entropic penalty associated with packing the long PS chains into HCP-ordered structures may lead to the narrowing of the HCP PS cylinder (C_{PS}) region in favor of the formation of micellar phases. Further, in Figure 4b, the complete disappearance of the C_{PS} region and unexpected narrowing of the lamellar window in mixtures with the f_{PS} = 0.73 copolymer compared to the less PS-rich copolymers also points to the role that packing frustration of PS chains may play in the rich lyotropic phase behavior of these materials. In block copolymer/selective molecular solvent mixtures, inversion of cylindrical phases has been widely reported. Inversion of cylindrical phases has been recently observed in PB-*block*-PEO/ionic liquid mixtures,[11] although the ionic liquids studied in these mixtures exhibit less selectivity compared to the S2VP/[Im][TFSI] system. It is anticipated that packing frustration of PS chains in the f_{PS} = 0.73 copolymer mixtures in combination with the strong selectivity of the ionic liquid for the P2VP block preclude formation of inverted cylindrical

Table 2. $f_{PS,eff}$ for Mixtures of [Im][TFSI] and S2VP Copolymers with Constant N_{P2VP}

f_{PS} of neat copolymer	χN[a]	$\phi_{P,C-L}$[b]	$f_{PS,eff}$[b]
0.42	24.6	0.85 ± 0.02	0.35 ± 0.01
0.49	28.9	0.78 ± 0.09	0.38 ± 0.04
0.62	35.6	0.67 ± 0.04	0.42 ± 0.02

[a] χN (T = 145 °C) was determined from ref 40. [b] Error in $\phi_{P,C-L}$ and $f_{PS,eff}$ is related to the range of ϕ_P separating lamellar and C_{PS} samples in Figure 4b.

phases on experimental time scales and instead lead to the formation of micelles with liquidlike order.

From Figure 4 it is observed that the ϕ_P at which the lamellae to C_{PS} lyotropic phase transition occurs, $\phi_{P,C-L}$, decreases monotonically as f_{PS} increases. The lamellar/C_{PS} phase boundary for a neat S2VP copolymer is determined by f_{PS} and the segregation strength, χN. The values of χN for the neat S2VP copolymers with constant N_{P2VP} as well as $\phi_{P,C-L}$ and $f_{PS,eff}$ for the mixtures with [Im][TFSI] are shown in Table 2, where $f_{PS,eff}$ is defined as the effective PS volume fraction at the $\phi_{P,C-L}$ phase transition and was calculated by assuming complete partitioning of the ionic liquid into the P2VP phase. Self-consistent mean-field theory predicts a lamellar/C_{PS} phase boundary between $0.32 \leq f_{PS} \leq 0.33$ for strongly segregated block copolymers and predicts the f_{PS} of this transition to decrease with increasing χN for χN less than about 30.[39] The neat copolymers in Table 2 span the weakly and strongly segregated regimes (χN ranges from 24.6 to 35.6). It is evident in Table 2 that $f_{PS,eff}$ for the mixtures is larger than the f_{PS} of the lamellar/C_{PS} phase boundary predicted for strongly segregated copolymers and that $f_{PS,eff}$ increases with increasing χN rather than decreasing with increasing χN as predicted for neat block copolymers for χN less than 30. It is probable that the addition of ionic liquid alters the statistical segment lengths of the two copolymer blocks, as has been observed in block copolymer/salt mixtures,[22] leading to this set of observations.

Domain Spacing. Theoretical[14] and experimental[14,17,41] studies have shown that the addition of a selective molecular solvent to a block copolymer increases d following the power law:

$$d \sim \phi_P^{\alpha} \tag{3}$$

where α is a measure of the solvent selectivity. Previously, the domain spacing of a symmetric S2VP block copolymer swollen with [Im][TFSI] was shown to increase according to eq 3 ($\alpha < 0$), indicating that the ionic liquid selectively solvates one block of the S2VP copolymer.[12] In Figure 5, a plot of d vs ϕ_P for lamellar mixtures of the constant N_{P2VP} copolymer series at 145 °C is shown to examine the effect of f_{PS} on α. The "affine dilution" limit describes the scenario in which the insoluble block is large compared to the solvated block. In this limit $\alpha = -1$ and the interfacial area per chain (A) remains constant upon the addition of solvent.[17] For a lamellar phase, A is given by

$$A = \frac{V}{d\phi_P} \tag{4}$$

where V is the volume of the insoluble phase. For mixtures containing the highly asymmetric S2VP(28.5−10.7) copolymer in [Im][TFSI], $\alpha = -1.1 \pm 0.1$. As f_{PS} decreases, the value of α becomes more negative, in stark contrast to observations of mixtures with molecular solvents.[17,42] On the basis of eqs 3 and 4 and values of $\alpha < -1$, A must decrease with decreasing ϕ_P, revealing that interfacial chain

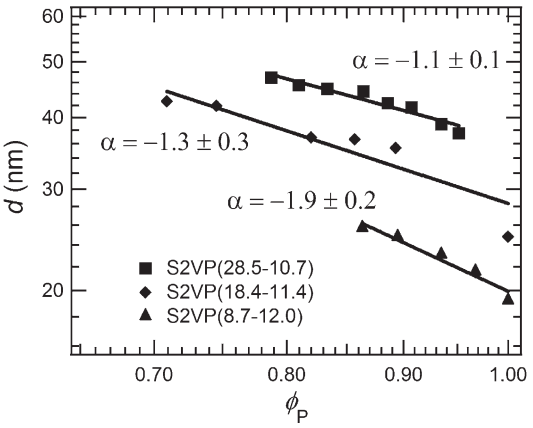

Figure 5. Lamellar domain spacing, d, vs ϕ_P determined from SAXS data at 145 °C. A power law, $d \sim \phi_P^{\alpha}$, is used to obtain α, and the errors represent one standard deviation of the fit.

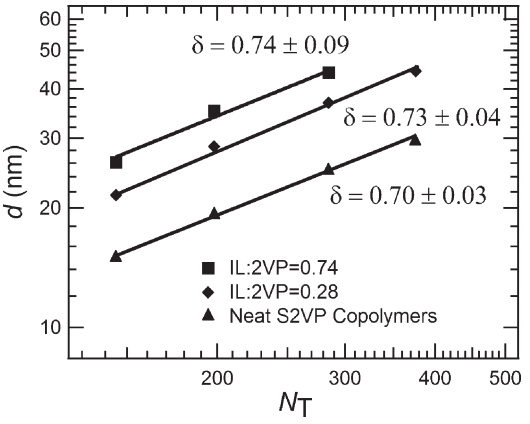

Figure 6. Lamellar domain spacing, d, vs N_T determined from SAXS data at 145 °C for S2VP copolymers with fixed N_{P2VP}, for the neat copolymer (▲), IL:2VP = 0.74 (■), and IL:2VP = 0.28 (◆). A power law fit, $d = \gamma N_T^{\delta}$, is used to obtain δ (reported errors are one standard deviation of the fit).

stretching perpendicular to the interface dominates over chain swelling parallel to the interface upon the addition of ionic liquid. While the origin of the increased segregation strengths compared to mixtures of block copolymers with molecular solvents cannot be definitively established from the current data set, it is anticipated that phase immiscibility is increased due to the presence of ions in the high dielectric P2VP phase, which comes about from a higher enthalpic free energy gain from ion solvation in the P2VP phase compared to the entropic penalty to confining the ions within a single phase.[23] The strong ion selectivity for the P2VP phase is supported by thermal characterization of the mixtures, in which the T_g of the P2VP phase decreases upon addition of [Im][TFSI] while the T_g of the PS phase remains in the vicinity of the neat T_g.

In Figure 6, the domain spacing of the neat S2VP copolymers with constant N_{P2VP} is shown to vary with N_T as $d = \gamma N_T^{\delta}$, where $\delta = 2/3$ within error, in agreement with strong segregation limit (SSL) scaling and experimental observations of the intermediate segregation regime[43−46] ($18 \leq \chi N \leq 47$ for the neat copolymers at 145 °C, as calculated from the Flory−Huggins temperature dependence suggested by Schulz et al.[40]). The prefactor, γ, is known to depend on morphology, f_{PS}, the ratio of the two statistical segment lengths (a_{PS}/a_{P2VP}), and χ.[43,44] Since the SSL scaling behavior of $d \sim N_T^{2/3}$ is also observed for fixed values of IL:2VP

as shown in Figure 6, where IL:2VP is the molar ratio of [Im][TFSI] to P2VP monomers, γ is a function of IL:2VP. In Table 3, γ is tabulated as a function of IL:2VP, where γ was calculated from power law fits to the data in Figure 6 with both γ and the N_T power law dependence (δ) used as fitting parameters. γ was found to increase monotonically with increasing IL:2VP. While the effective χ is expected to increase with increasing IL:2VP based on the highly negative values of α observed, further studies of chain statistical dimensions are necessary to quantitatively estimate the effective χ from the domain spacing data.

Thermotropic Phase Behavior. It is anticipated that addition of [Im][TFSI] will increase the T_{ODT} of neat S2VP copolymers due to increased segregation strength of the system. In Figure 7a, SAXS profiles are shown for the neat, lamellar S2VP(4.9−6.6) copolymer at varying temperatures. An ODT is evident at 185 ± 20 °C based on the discontinuous change in the full width at half-maximum (fwhm) and intensity of the q^* peak shown in Figure 7b. The ODT is fully reversible upon cooling and in close agreement with the predicted T_{ODT} (197 °C) of a f_{PS} = 0.50, N_T = 110 copolymer (as calculated from the Flory−Huggins temperature dependence suggested by Schulz et al.[40]). In Figure 7c, SAXS profiles for S2VP(4.9−6.6)/[Im][TFSI] mixtures for varying ϕ_P at 225 °C are shown. The profiles are remarkably similar to those observed at 145 °C (Figure 3b) and indicate that across a wide range of ϕ_P the ordered block copolymer phase is stabilized with respect to temperature by the presence of ionic liquid. While the origin of the increased T_{ODT} in the S2VP/[Im][TFSI] system cannot be definitively established from the current, limited data set, such behavior could result from one or both of the following possibilities: (1) the PS and P2VP interaction parameters with [Im][TFSI] are strongly temperature-dependent or (2) as observed from domain scaling analysis, the S2VP/[Im][TFSI] mixtures have increased segregation strength compared to the neat S2VP copolymer due to the enthalpically driven presence of ions in the P2VP phase.

Table 3. γ as a Function of IL:2VP

IL:2VP	γ^a
0.00	0.48 ± 0.07
0.28	0.59 ± 0.12
0.74	0.68 ± 0.35

[a] Error in γ is one standard deviation of the fit.

Conclusions

The phase behavior of S2VP/[Im][TFSI] mixtures for copolymers with a wide range of f_{PS} and N_T was studied using SAXS, SANS, and DSC. The observed dependence of the P2VP/[Im][TFSI] phase T_g on IL:2VP was found to be independent of f_{PS} and N_T of the copolymer and cannot be predicted by standard theories for the thermal properties of polymer/molecular solvent mixtures. SAXS and SANS characterization revealed the existence of lamellar, cylindrical, ordered micellar, and disordered micellar phases, in agreement with studies of block

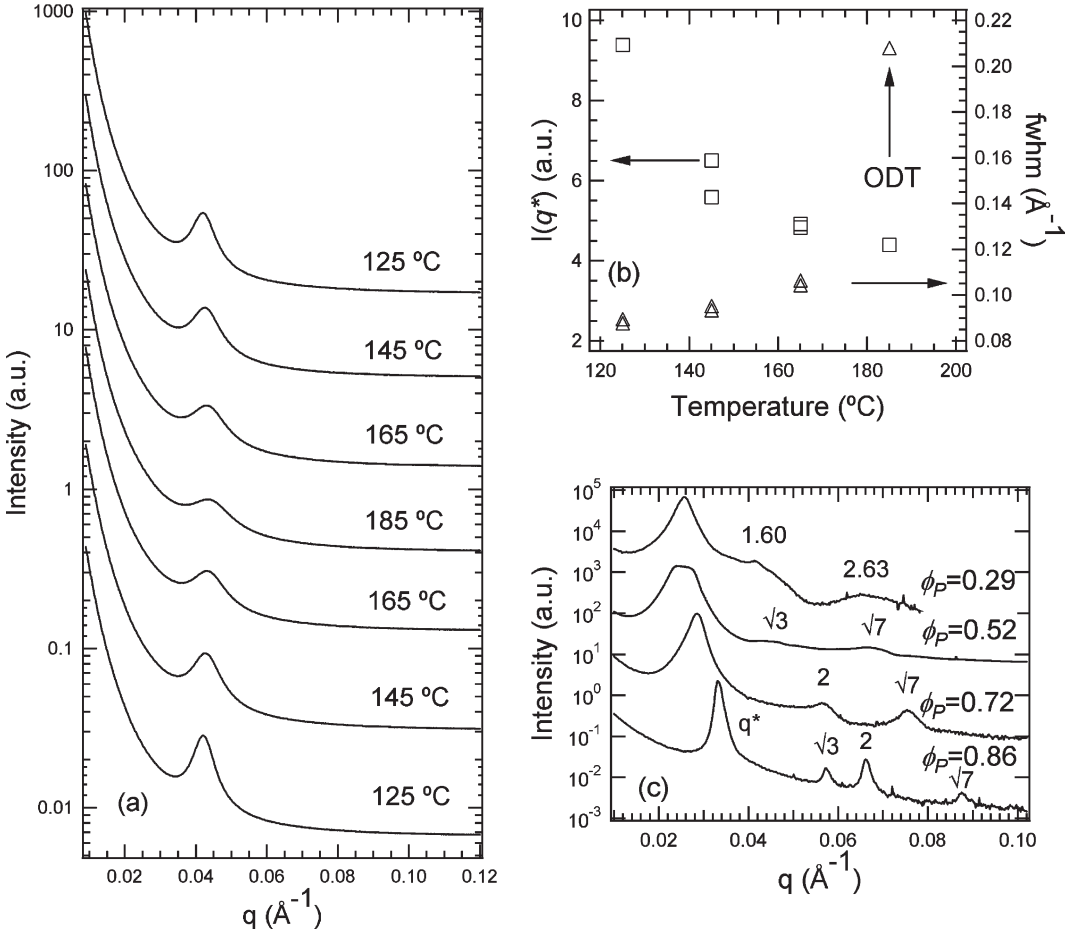

Figure 7. (a) SAXS profiles (offset for clarity) of ϕ_P = 1.00, S2VP(4.9−6.6) at varying temperatures. (b) Plot of $I(q^*)$ (□) and fwhm (Δ) vs temperature (°C) of ϕ_P = 1.00, S2VP(4.9−6.6). The ODT is defined as the point at 185 ± 20 °C, and overlapping data points at a given temperature were recorded upon heating and cooling. (c) SAXS profiles (offset for clarity) of S2VP(4.9−6.6)/[Im][TFSI] mixtures at varying ϕ_P at 225 °C.

copolymer/selective molecular solvent mixtures. Scaling analysis of the S2VP/[Im][TFSI] mixtures revealed a decrease in the interfacial area occupied by each S2VP chain upon the addition of ionic liquid, which indicates an increase in segregation strength upon the addition of ionic liquid that is larger than previous observations of block copolymer/selective molecular solvent mixtures and is due to the enthalpically driven presence of ions in the high dielectric P2VP phase. Across a broad range of IL:2VP ratios, d of the mixtures was found to follow the molecular weight scaling predicted by SSL theory. An increase in the T_{ODT} of the S2VP/[Im][TFSI] mixtures compared to the neat copolymer was in qualitative agreement with the scaling analysis.

Acknowledgment. We gratefully acknowledge support from the Assistant Secretary for Energy Efficiency and Renewable Energy, Office of Hydrogen, Fuel Cell, and Infrastructure Technologies of the U.S. Department of Energy under Contract DE-AC02-05CH11231. The authors thank Dr. John Kerr for useful discussions. SAXS experiments were performed at the Advanced Light Source and the Stanford Synchrotron Radiation Lightsource, and SANS experiments were conducted at Oak Ridge National Laboratory's (ORNL) High Flux Isotope Reactor. All three are national user facilities supported by the Department of Energy, Office of Basic Energy Sciences. We gratefully acknowledge Dr. Alexander Hexemer, Dr. Cheng Wang, and Dr. Eric Schaible for experimental assistance at the ALS, Dr. John Pople for experimental assistance at the SSRL, and Alisyn Nedoma, Dr. Yuri Melnichenko, and Dr. Gang Cheng for experimental assistance at ORNL.

Supporting Information Available: Representative DSC heating scans and SAXS and SANS profiles of additional S2VP/[Im][TFSI] mixtures. This material is available free of charge via the Internet at http://pubs.acs.org.

References and Notes

(1) Wasserceid, P.; Welton, T. *Ionic Liquids in Synthesis*; Wiley-VCH Verlag: Weinheim, 2003.
(2) Noda, A.; Susan, M. A. B. H.; Kudo, K.; Mitsushima, S.; Hayamizu, K.; Watanabe, M. *J. Phys. Chem. B* **2003**, *107* (17), 4024–4033.
(3) Doyle, M.; Choi, S. K.; Proulx, G. *J. Electrochem. Soc.* **2000**, *147* (1), 34–37.
(4) Fernicola, A.; Panero, S.; Scrosati, B.; Tamada, M.; Ohno, H. *ChemPhysChem* **2007**, *8* (7), 1103–1107.
(5) Matsuoka, H.; Nakamoto, H.; Susan, M. A. B. H.; Watanabe, M. *Electrochim. Acta* **2005**, *50* (19), 4015–4021.
(6) Sekhon, S. S.; Lalia, B. S.; Park, J. S.; Kim, C. S.; Yamada, K. *J. Mater. Chem.* **2006**, *16* (23), 2256–2265.
(7) Cho, J. H.; Lee, J.; Xia, Y.; Kim, B.; He, Y. Y.; Renn, M. J.; Lodge, T. P.; Frisbie, C. D. *Nature Mater.* **2008**, *7* (11), 900–906.
(8) Lee, J.; Panzer, M. J.; He, Y. Y.; Lodge, T. P.; Frisbie, C. D. *J. Am. Chem. Soc.* **2007**, *129* (15), 4532–+.
(9) Kim, G. T.; Appetecchi, G. B.; Alessandrini, F.; Passerini, S. *J. Power Sources* **2007**, *171* (2), 861–869.
(10) Sakaebe, H.; Matsumoto, H. *Electrochem. Commun.* **2003**, *5* (7), 594–598.
(11) Simone, P. M.; Lodge, T. P. *Macromolecules* **2008**, *41*, 1753–1759.
(12) Virgili, J. M.; Hexemer, A.; Pople, J. A.; Balsara, N. P.; Segalman, R. A. *Macromolecules* **2009**, *42* (13), 4604–4613.
(13) Hanley, K. J.; Lodge, T. P. *J. Polym. Sci., Part B: Polym. Phys.* **1998**, *36* (17), 3101–3113.
(14) Hanley, K. J.; Lodge, T. P.; Huang, C.-I. *Macromolecules* **2000**, *33* (16), 5918–5931.
(15) Huang, C. I.; Hsueh, H. Y. *Polymer* **2006**, *47* (19), 6843–6856.
(16) Huang, C.-I.; Lodge, T. P. *Macromolecules* **1998**, *31* (11), 3556–3565.
(17) Lai, C.; Russel, W. B.; Register, R. A. *Macromolecules* **2002**, *35* (10), 4044–4049.
(18) Lai, C.; Russel, W. B.; Register, R. A. *Macromolecules* **2002**, *35* (3), 841–849.
(19) Ruzette, A. V. G.; Soo, P. P.; Sadoway, D. R.; Mayes, A. M. *J. Electrochem. Soc.* **2001**, *148* (6), A537–A543.
(20) Epps, T. H.; Bailey, T. S.; Pham, H. D.; Bates, F. S. *Chem. Mater.* **2002**, *14* (4), 1706–1714.
(21) Lee, D. H.; Kim, H. Y.; Kim, J. K.; Huh, J.; Ryu, D. Y. *Macromolecules* **2006**, *39* (6), 2027–2030.
(22) Wang, J.-Y.; Chen, W.; Russell, T. P. *Macromolecules* **2008**, *41* (13), 4904–4907.
(23) Wang, Z. G. *J. Phys. Chem. B* **2008**, *112* (50), 16205–16213.
(24) He, Y. Y.; Li, Z. B.; Simone, P.; Lodge, T. P. *J. Am. Chem. Soc.* **2006**, *128* (8), 2745–2750.
(25) Yokoyama, H.; Mates, T. E.; Kramer, E. J. *Macromolecules* **2000**, *33* (5), 1888–1898.
(26) Virgili, J. M.; Nedoma, A. J.; Segalman, R. A.; Balsara, N. P.; *Macromolecules* **2010**, *43*, 3750−3756.
(27) Wignall, G. D.; Bates, F. S. *J. Appl. Crystallogr.* **1987**, *20*, 28–40.
(28) Lodge, T. P.; Hamersky, M. W.; Hanley, K. J.; Huang, C. I. *Macromolecules* **1997**, *30* (20), 6139–6149.
(29) Gordon, M.; Taylor, J. S. *J. Appl. Chem.* **1952**, *2* (9), 493–500.
(30) Fox, T. G. *Bull. Am. Phys. Soc.* **1956**, *1*, 123.
(31) Susan, M. A.; Kaneko, T.; Noda, A.; Watanabe, M. *J. Am. Chem. Soc.* **2005**, *127* (13), 4976–4983.
(32) Mcconnell, G. A.; Gast, A. P.; Huang, J. S.; Smith, S. D. *Phys. Rev. Lett.* **1993**, *71* (13), 2102–2105.
(33) Laughlin, R. G. *The Aqueous Phase Behavior of Surfactants*; Academic Press: San Diego, 1994.
(34) Meli, L.; Lodge, T. P. *Macromolecules* **2009**, *42* (3), 580–583.
(35) Cavicchi, K. A.; Lodge, T. P. *J. Polym. Sci., Part B: Polym. Phys.* **2003**, *41* (7), 715–724.
(36) McConnell, G. A.; Gast, A. P. *Macromolecules* **1997**, *30* (3), 435–444.
(37) Halperin, A.; Tirrell, M.; Lodge, T. P. *Adv. Polym. Sci.* **1992**, *100*, 31–71.
(38) Zhang, L. F.; Eisenberg, A. *Polym. Adv. Technol.* **1998**, *9* (10−11), 677–699.
(39) Cochran, E. W.; Garcia-Cervera, C. J.; Fredrickson, G. H. *Macromolecules* **2006**, *39* (7), 2449–2451.
(40) Schulz, M. F.; Khandpur, A. K.; Bates, F. S.; Almdal, K.; Mortensen, K.; Hajduk, D. A.; Gruner, S. M. *Macromolecules* **1996**, *29* (8), 2857–2867.
(41) Shibayama, M.; Hashimoto, T.; Kawai, H. *Macromolecules* **1983**, *16* (1), 16–28.
(42) Hajduk, D. A.; Kossuth, M. B.; Hillmyer, M. A.; Bates, F. S. *J. Phys. Chem. B* **1998**, *102* (22), 4269–4276.
(43) Semenov, A. N. *Macromolecules* **1989**, *22* (6), 2849–2851.
(44) Lipic, P. M.; Bates, F. S.; Matsen, M. W. *J. Polym. Sci., Part B: Polym. Phys.* **1999**, *37* (16), 2229–2238.
(45) Whitmore, M. D.; Vavasour, J. D. *Acta Polym.* **1995**, *46* (5), 341–360.
(46) Almdal, K.; Rosedale, J. H.; Bates, F. S.; Wignall, G. D.; Fredrickson, G. H. *Phys. Rev. Lett.* **1990**, *65* (9), 1112–1115.